



Calculation of Acoustic Green's Function using BEM and Dirichlet-to-Neumann-type boundary conditions

Adrian R.G. Harwood¹; Iain D.J. Dupère²

School of Mechanical, Aerospace & Civil Engineering
The University of Manchester
Sackville Street
Manchester
M1 3BB, United Kingdom

ABSTRACT

Hybrid computational aero-acoustic (CAA) solution schemes rely on the knowledge of a scattering function known as a Green's function to propagate source fluctuations to the far-field. Presently, these schemes are restricted to relatively simple geometries. We present here a computational method for evaluating Green's functions within more geometrically complex regions, as a means of extending the versatility of existing hybrid schemes. The direct collocation implementation of the Boundary Element Method used in truncated, semi-infinite domains, introduces additional unknowns on the boundary. In this paper we develop a modified boundary element formulation to efficiently incorporate approximate Non-Reflecting Boundary Conditions for an arbitrary number of truncation boundaries. The boundary condition is based on the Dirichlet-to-Neumann mapping operator. Results are compared to known analytical Green's functions for an infinite pipe as a means of validating the new code. The method achieves relative errors of less than 1% compared with the analytical solution for the highest mesh density tested. Execution time, known to be large for acoustic problems, is minimised through the use of multi-threading.

Keywords: BEM, DtN Operator, Green's Functions
I-INCE Classification of Subjects Number(s): 23.6

1. INTRODUCTION

The prediction of noise generated by an aero-acoustic source has been the subject of research since the 1950s and may be broadly seen to consist of two fundamental tasks: the computation of source characteristics; and the propagation of the calculated acoustic fluctuations to an observer. Hybrid noise prediction schemes combine the strengths of both numerical and analytical schemes in a multi-domain set-up [1]. A useful summary may be found in the review by Singer *et al.* [2]. Use of these schemes as an alternative to solely numerical procedures precludes the need to mesh and solve equations in the region between the source and the observer meaning the demand on computational resources is significantly less. However, hybrid schemes generally rely on the evaluation of an integral equation for the propagation step whose kernel consists of a Green's function. This Green's function must satisfy the boundary conditions in the propagation domain. Analytical representations of exact Green's functions are few and far between, despite there being a number of published approximations [3]. Hence we are limited to propagating sound using integral equations in regions where Green's functions are available. In order to extend the versatility of existing hybrid CAA schemes, we develop here a suitable means to accurately and robustly compute acoustic Green's functions in geometries where analytical representations are unavailable. Resulting hybrid schemes may therefore propagate the sound directly in a single step, using a numerical representation of the Green's function, without the need for an intermediate domain or additional calculation to find the scattered component of the acoustic field.

¹adrian.harwood@manchester.ac.uk

²iain.dupere@manchester.ac.uk

This paper examines the use of the Boundary Element Method (BEM) for this purpose. Specifically, we focus on a particularly useful class of 2D problems – acoustic scattering in a channel with or without geometrical obstructions. Such problems are typically dominated by 2D effects and their role in sound attenuation has been observed for some time. Although the treatment in this paper is limited to 2D problems, the principles are easily extended to three dimensions. The typical version of the direct BEM formulation used in this paper, requires a closed boundary on which either the solution variable or its normal derivative is known on every segment of the boundary. For the semi-infinite class of domains we presently examine, such information is not readily available resulting in an under-determined set of equations. We truncate the channel in both the upstream and downstream directions, then specify a non-reflecting boundary condition (NRBC) on these boundaries which simultaneously closes the BEM system mathematically. This boundary condition is a non-local boundary condition, which demonstrate greater accuracy than local approximations [4]. However, non-local boundary conditions are generally more computationally expensive due to the coupling of every node on the boundary surface. Furthermore, the computation of a large number of integrals is usually required. We show in this paper that the inclusion of a non-local boundary condition in the constant element direct BEM avoids the additional numerical integration entirely, and thus allows an accurate truncation of the BEM domain at little cost.

2. GREEN'S FUNCTION FOR THE HELMHOLTZ EQUATION

Time-harmonic acoustic problems, in the absence of a mean flow, may be represented by a Helmholtz BVP of the form

$$(\nabla^2 + k^2)\hat{\phi}(\mathbf{x}, \omega) = -\hat{q}(\mathbf{x}, \omega) \quad \text{in } \Omega \quad (1a)$$

$$\hat{\phi}(\mathbf{x}, \omega) = g(\omega) \quad \text{on } \Gamma_1 \quad (1b)$$

$$\frac{\partial \hat{\phi}}{\partial n}(\mathbf{x}, \omega) = h(\omega) \quad \text{on } \Gamma_2 \quad (1c)$$

In the most general case we assume the source term to be a function of spatially compact support. One method of developing an analytical solution to this BVP is to transform the differential equation into an integral equation in which we can substitute the boundary conditions. These boundary conditions are incorporated in the Green's function $\hat{G}(\mathbf{x}, \mathbf{y}, \omega)$, where \mathbf{y} refers to the compact source coordinate. This is the solution to the singular form of the original differential equation (Equation (2)) and satisfies the original boundary conditions. Physically, it may be interpreted as an outgoing wave produced by an impulsive unit point source at \mathbf{y} .

$$(\nabla^2 + k^2)\hat{G}(\mathbf{x}, \mathbf{y}, \omega) = \delta(\mathbf{x} - \mathbf{y}) \quad (2)$$

In the absence of boundary conditions we may consider this wave to propagate in free-space and hence we often use the free-space Green's function, readily available analytical form. However, the introduction of boundaries and hence associated boundary conditions complicate matters as an analytical representation of \hat{G} is difficult to construct. In the remainder of this paper we show that the BEM can be a robust and accurate means of numerically computing Green's functions within arbitrary geometries. We now develop a BEM formulation suitable for solving a class of two-dimensional BVPs.

3. DIRECT COLLOCATION BOUNDARY ELEMENT FORMULATION

When analysing problems on infinite domains, the Boundary Element Method (BEM) offers a number of advantages over the Finite Element Method (FEM) (see for example [5, 6]). A number of different BEM formulations exist depending on the type of boundary reduction procedure used. The direct formulation is arguably the simplest to derive and implement with many introductory texts on the subject of BEM focussing on this formulation in particular. For this reason, we use this implementation here.

The direct boundary integral equation (BIE) representation of the general BVP (Equation (3)) where, for convenience, we have dropped the hat notation, is given below. The derivative of the solution ϕ with respect to the outward normal is represented by the symbol ψ . This considers a problem where the boundary is closed and comprises three different types of boundary characterised by the

information known on the particular boundary segment: Γ_1 -type (type 1) boundaries contain known values of ϕ , Γ_2 -type (type 2) boundaries contain known values of ψ . We also consider an extension to this problem where we also have Γ_3 -type (type 3) boundaries which are truncation boundaries and hence contain no known information (Figure 1).

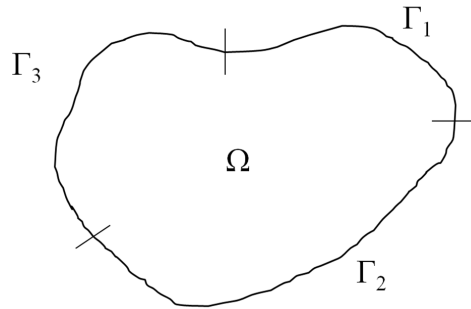


Figure 1 – General 2D BVP geometry with the boundary segmented into those of type 1, type 2 and type 3.

The traditional formulation of the BEM, based on Equation (3), is soluble while some information about the solution is known at each node on the boundary.

Considering for the moment the case where all segments of the boundary may be classified as either type 1 or type 2, application of the weighted residual method produces the usual BIE Equation (3) where ϕ^* and ψ^* represent the free-space Green's function and its normal derivative for the homogeneous BVP in free-space. The overbar signifies a known quantity.

$$c\phi + \int_{\Gamma_2} \phi\psi^* d\Gamma + \int_{\Gamma_1} \bar{\phi}\psi^* d\Gamma = \int_{\Gamma_2} \bar{\psi}\phi^* d\Gamma + \int_{\Gamma_1} \psi\phi^* d\Gamma \quad (3)$$

This statement is discretised into constant elements giving for the i -th fundamental solution position

$$c_i\phi_i + \sum_{j=1}^N \left(\int_{\Gamma_j} \psi_j^* d\Gamma \right) \phi_j = \sum_{j=1}^N \left(\int_{\Gamma_j} \phi_j^* d\Gamma \right) \psi_j \quad (4)$$

which we represent in matrix form as

$$\mathbf{H}\vec{\phi} = \mathbf{G}\vec{\psi} \quad (5)$$

This formulation is soluble since type 1 and type 2 boundaries specify either ϕ or ψ at each node of the boundary, resulting in only a single unknown per element.

If we now introduce a segment of type 3 boundary as part of the problem consisting of K elements, the system becomes under-determined. One means of addressing this to eliminate one set of unknowns through the introduction of additional equations which relate the two unknowns for each element on the type 3 boundary. In this case we end up with a system whose i -th component is

$$c_i\phi_i + \sum_{j=1}^N \left(\int_{\Gamma_j} \psi_j^* d\Gamma \right) \phi_j = \sum_{j=1}^{N-K} \left(\int_{\Gamma_j} \phi_j^* d\Gamma \right) \psi_j + \sum_{j=1}^K \left(\int_{\Gamma_j} \phi_j^* d\Gamma \right) \psi_j \quad (6)$$

Now for all values of $j \in K$ we have two unknowns. What we require therefore, is to eliminate the unknown values ψ_j by using an equation which maps values of $\psi_j \mapsto \phi_j$ for $j \in K$. We call this mapping a DtN map or DtN operator.

4. DIRICHLET-TO-NEUMANN OPERATOR

In order to fully determine the system of equations in the previous BEM formulation Equation (6), we require an additional set of equations which relate ϕ to ψ on the artificial boundary. Global NRBCs based on the Dirichlet-to-Neumann operator [4] meet the requirements; using the DtN operator, the solution ϕ may be mapped to its normal derivative ψ . If applied at every node on the artificial boundary, enough additional equations are generated to close Equation (6). The DtN

operator is constructed by considering the solution to the homogeneous BVP in the region beyond the truncation boundary, be that upstream or downstream. Knowledge of an analytical general solution in this region, evaluated on the truncation boundary is therefore equivalent to the solution of the interior problem on the same boundary as away from the source point (or source region if source is distributed) the two BVPs should be equivalent. Since the construction of the DtN operator requires knowledge of a specific solution homogeneous solution characterized by the type of geometry beyond the truncation boundary, it is necessary to restrict ourselves in this paper to a subset of the general class of problem in which the domains beyond the truncation boundaries are those of rectangular channels or ducts (Figure 2) [7].

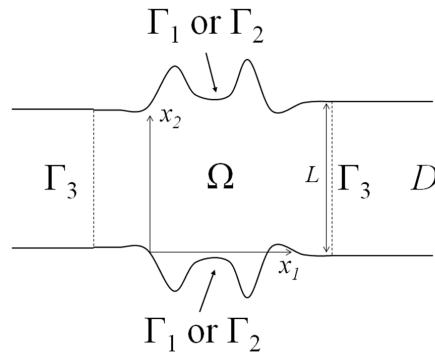


Figure 2 – An arbitrary 2D waveguide which is assumed to be a parallel-sided 2D waveguide beyond truncation boundaries denoted Γ_3

The problem domain, in which the BVP defined by Equation (1) applies, is defined by Ω and the infinite analytical domain in which the homogeneous version applies in D . Since we are dealing with a waveguide, it is appropriate to express the vector position \mathbf{x} in terms of its scalar components $[x_1, x_2]$. We drop the frequency dependence for convenience from the propagating wave number $\gamma_n \equiv \gamma_n(\omega)$ in the following derivation. The solution to the problem in D subject to rigid-wall boundary conditions on the upper and lower walls is therefore given by the function $\bar{\phi}(x_1, x_2)$ which, using separation of variables, may be represented by an eigenfunction expansion (Fourier series representation) in the cross-duct direction multiplied by a single outgoing wave function centred on the truncation boundary at \bar{x}_1 as:

$$\begin{aligned} \bar{\phi}(x_1, x_2) &= \phi_1(x_1)\phi_2(x_2) \\ &= \left[a_0 + \sum_{n=1}^{\infty} a_n \cos\left(\frac{n\pi x_2}{L}\right) \right] e^{\pm i\gamma_n|x_1 - \bar{x}_1|} \end{aligned} \quad (7a)$$

Where the coefficients are the usual Euler formulae for the cross-duct Fourier series

$$a_0 = \frac{1}{L} \int_0^L \phi_2(x_2) dx_2 \quad (7b)$$

$$a_n = \frac{2}{L} \int_0^L \phi_2(x_2) \cos\left(\frac{n\pi x_2}{L}\right) dx_2 \quad (7c)$$

We can differentiate this with respect to the outward normal to the truncation boundary to get an expression for ψ as:

$$\begin{aligned} \frac{\partial \phi}{\partial x_1}(x_1, x_2) &\equiv \psi(x_1, x_2) \\ &= \pm i\gamma_0 a_0 e^{i\gamma_0|x_1 - \bar{x}_1|} \pm i \sum_{n=1}^{\infty} \gamma_n a_n \cos\left(\frac{n\pi x_2}{L}\right) e^{\pm i\gamma_n|x_1 - \bar{x}_1|} \end{aligned} \quad (8)$$

This relationship may then be used as the definition of DtN operator M defined as

$$\psi(x_1, x_2) = M[\phi(x_1, x_2)]$$

Our analysis is equivalent to the 2D rigid wall expressions of Harari *et al.* [7].

5. BEM IMPLEMENTATION

The DtN boundary condition (Equation (8)) is exact. However, we should note that practical implementation requires us to truncate the infinite series and hence this exactness is lost. Furthermore, the waves absent from the series essentially have a boundary condition $\partial/\partial n = 0$ which generates reflections on the boundary for these modes but also can cause mathematical issues of non-uniqueness [8]. One solution is to ensure the number of terms in the DtN condition is large enough to include all modes required for the solution to the problem to be unique. However, particularly for higher-dimensional problems and problems involving high frequency propagation, the series representation may contain a large number of terms, many of which are included to ensure uniqueness rather than to improve the accuracy by any appreciable amount [9]. The modified DtN formulation of Grote and Keller [8] which imposes the radiation condition on these missing modes instead, is a more practical and alternative.

Wave-guide problems afford a certain degree of simplification of the issue of uniqueness and reflection caused by truncation of the DtN series. In a wave-guide, the propagating modes are restricted based on the relationship between frequency and duct geometry. Since the boundary condition $\partial/\partial n = 0$ is exact for the cut-off modes, Harari *et al.* [7] have shown that we only require at least the propagating modes in the boundary condition expansion in order for a unique solution to be guaranteed. Our truncation boundaries are placed far enough from the source to ensure all evanescent modes have suitably decayed by the truncation boundary. Therefore, the standard DtN containing a relatively few number of terms is sufficient for both uniqueness and accuracy.

To incorporate the DtN relationship into the boundary element formulation we introduce the discrete representation of the solution on the truncation boundary into Equation (8). We label the values of ϕ_j over the outlet $j \in K$ ϕ_k . The manipulation of the coefficient integrals then uses the fact that since we have used constant (discontinuous) boundary elements, the values of ϕ_k are constant over each element on the truncation boundary. The values of ϕ_k may be brought outside the integrals with the remaining integral simple to compute analytically.

$$a_0 = \frac{1}{L} \sum_k \frac{\phi_k}{e^{\pm i\gamma_n |x_1 - \tilde{x}_1|}} l_k$$

where l_k is the length of the k -th element. Similarly the other integral becomes:

$$a_n = \frac{2}{L} \sum_k \frac{\phi_k}{e^{\pm i\gamma_n |x_1 - \tilde{x}_1|}} \frac{L}{n\pi} \Delta_{nk}$$

where $\Delta_{nk} = \left[\sin\left(\frac{n\pi b_k}{L}\right) - \sin\left(\frac{n\pi a_k}{L}\right) \right]$ in which $[a_k, b_k]$ are the coordinates of the endpoints of the k -th element in the x_2 -direction. We may now substitute for the ϕ_k values on the truncation boundary and rearrange the system which results in a reduction in the elements of $\mathbf{G}\vec{\psi}$ and a correction of the elements of \mathbf{H} . The modifications are summarised as

$$h_{ij} \mapsto h_{ij} - \sum_k g_{ik} \delta_{jk} \quad (9a) \quad \beta_{nj} = \frac{2i\gamma_n}{\pi} \frac{\Delta_{nj}}{n} \quad (9d)$$

$$\delta_{jk} = \alpha_j + \sum_n \beta_{nj} \Psi_{nk} \quad (9b) \quad \Psi_{nk} = \cos\left(\frac{n\pi(x_2)_k}{L}\right) \quad (9e)$$

$$\alpha_j = \frac{ikl_j}{L} \quad (9c) \quad \Delta_{nj} = \left[\sin\left(\frac{n\pi b_j}{L}\right) - \sin\left(\frac{n\pi a_j}{L}\right) \right] \quad (9f)$$

This fully determines the system which can now be solved for all the missing values on the type 1 and type 2 boundaries and the ϕ values on the type 3 boundary. The corresponding values of ψ on the type 3 boundary may then be found from the discretised equation

$$\psi_i = \pm \frac{ik}{L} \sum_k \phi_k l_k \pm \frac{2i}{\pi} \sum_k \left[\left(\sum_k \frac{\phi_k \delta_{nk}}{n} \right) \gamma_n \cos \left(\frac{n\pi\gamma_i}{L} \right) \right] \quad (10)$$

In the context of the discussion in the introduction we note that this boundary condition is non-local in the sense that it couples all the unknowns on the truncation boundary. Due to the already full nature of the BEM matrix as well as the lack of numerical integration for constant boundary elements, this non-locality not the disadvantage it is made out to be in many publications concerned with the application of DtN to FEM. The implementation procedure is easily repeated for an arbitrary number of separate truncation boundaries.

6. RESULTS

Having established an extended BEM to approximate solutions to BVPs in semi-infinite domains, we now determine how the number of terms in the DtN map affects the accuracy and execution time and whether they are affected by any notable interactions between the choice of number of terms, mesh density and frequency. The mesh density may assist in filtering out unsupported reflected modes from the boundary condition but also may fail to allow unsupported transmitted modes through the boundary, which would contaminate the solution. We compute here the Green's function for a rigid wave guide using the BEM formulation stated above. We present and analyse the effects of changing the mesh density, DtN expansion terms and frequency on the accuracy and execution time.

6.1 2D Green's Function for a Rigid Channel

We consider the Green's function for an acoustically rigid channel of width d . The geometry beyond the problem domain is assumed to continue to be that of an acoustically rigid, straight-walled channel. The analytical solution to this problem for a source position (ξ, η) , observer position (x, y) and origin located on the lower surface of the channel is given by [10]

$$G(X, y, \eta) = -\frac{1}{2} \sum_{m=0}^{\infty} \epsilon_m \frac{e^{-\gamma_{2m}|X|/d}}{\gamma_{2m}} \cos \frac{m\pi y}{d} \cos \frac{m\pi \eta}{d}$$

where

$$\gamma_m = -i \left(k^2 d^2 - \frac{m^2 \pi^2}{4} \right)^{0.5} \quad \epsilon_m = \begin{cases} 1 & \text{if } m = 0 \\ 2 & \text{otherwise} \end{cases} \quad \text{and } X = x - \xi$$

This solution is evaluated using 5000 terms of the infinite series which gives an accuracy to at least 5 significant figures [10]. Errors will therefore be of the same order of magnitude as the threshold of hearing (2×10^{-5}). We choose to fix the location of the boundaries arbitrarily at $x = \pm 3d$.

6.1.1 Range Selections

For our numerical experiments we select the audible frequency range from $f = 20$ to 20,000 Hz. We initially stipulate a required absolute accuracy corresponding the threshold of hearing (of the order 10^{-5}). In reality, for noise calculations, this need not be so stringent as audible error noise even an order of magnitude greater would likely be quiet enough to not attract attention. However, there are many situations where even relatively low amplitude acoustics can excite instabilities in fluid flow which generate feedback loops or other forms of radiation [11]. If our numerical Green's functions were used in such cases, the low amplitude numerical error may impact significantly. In order to determine a range of mesh density selections n which will resolve the waves at frequency f and achieve the desired accuracy, we compare the exact integral of a single cycle of wavelength λ_f to the same integral computed using constant BEM of mesh density n . The number of elements required to achieve errors of 10^{-5} is impractical ($n = 400/\lambda_f$), requiring memory of the order 10^2 GB which is not widely available. A more modest target of 8 elements per wavelength is selected, which achieves an absolute error in the amplitude of the order 10^{-2} , a relative error of less than 10%. Therefore, mesh density varies from $n = 10$ to $n = 500$ to ensure a mixture of good and poor resolution across the range of source frequencies. This upper limit has the added benefit of being able to resolve all the propagating waves at the highest frequency f .

The choice of DtN terms in the expansion on the truncation boundary should allow us to investigate results for both resolved and unresolved DtN waves. We choose to vary the number of DtN terms in the expansion from $M = 10$ to 250, where the upper limit is beyond the resolution capabilities of the

mesh. As discussed earlier, the exclusion of propagating modes in the DtN series at the artificial boundary results in essentially setting a boundary condition equal to zero for those modes. Unwanted reflections are thus inevitable if either the DtN expansion does not support the appropriate number of propagating modes or the boundary is close enough to the source that the cut-off higher-order modes have not sufficiently decayed. This latter situation is only expected at lower frequencies for our chosen boundary position. The justification of this expectation is omitted here due to space restrictions.

In all cases tested, after computing the boundary values, the code proceeds to evaluate the solution over a line of 120 points. All error values are mean values over this grid. This is considered a fairer representation of the accuracy of the calculation than considering the maximum error as errors near the singularity and near boundaries are expected to be larger than elsewhere in the domain. Since these regions occupy only a small percentage of the overall region of interest their error values in isolation are not a suitable measure.

6.1.2 Accuracy variation with Frequency

We start by examining the variation in RMS relative error with frequency for different combinations of M and n . Errors can arise from several sources: the poor resolution of the source waves at all boundaries; the lack of terms in the DtN boundary condition; poor resolution of the DtN waves at the artificial boundary; or the poor performance of internal point valuation by the BEM when the point is near the singularities in the fundamental solution at the boundary. Figures 3a and 3b show the variation in error over the range of f and M for two values of n . As can be easily observed, a sudden jump in error is evident as an increase in frequency cuts-on higher-order modes not capable of being represented by the boundary conditions of lower M . This behaviour is consistent with the results of Harari *et al.* [7] who state that accuracy of the DtN condition is ensured by including all the propagating modes in the expansion. This source of error is the most significant.

For the higher values of n , the error ramps up with source frequency f rather than jumps. This suggests that the exclusion of propagating modes is more detrimental at the lower resolutions. If the frequency is increased further, there comes a point beyond which further exclusion of modes has no dramatic effect, with a relatively uniform increase in error attributed to the increasingly poor resolution of higher frequency waves. Likewise, the inclusion of increasing numbers of evanescent modes also has little effect on the accuracy, even at low frequencies. This is due to the rapid decay of such modes and the placement of our downstream boundary such that the magnitude of these waves are negligible.

In contrast, the inclusion of propagating modes into the DtN expansion at the lowest mesh resolution has little effect on the error variation with frequency. For all but the first frequency the poor resolution is the principal source of error with inclusion of propagating modes having little benefit if they are poorly resolved. Therefore, we can conclude that if resolution is adequate, the principal source of error with frequency relates to the inclusion of propagating modes in the DtN expansion, with poor resolution of the waves in the field responsible for a more general increase in error with frequency.

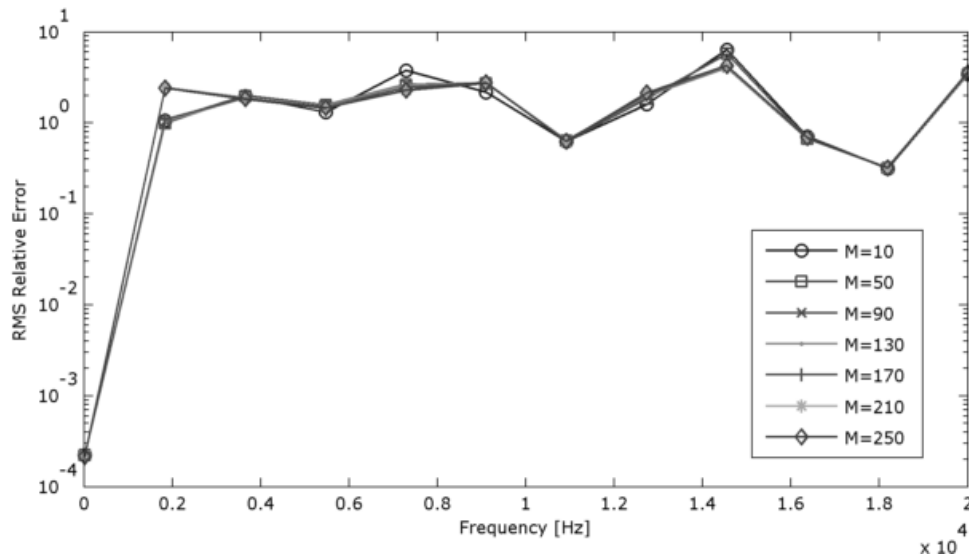
6.1.3 Accuracy variation with Mesh Density

In general, the error decreases with mesh density. This behaviour is strongly influenced by the inclusion of enough terms in the DtN expansion such that M is large enough to allow all propagating cross-channel modes to be represented. However, there are some instances, where for a given combination of f and M a ‘spike’ is observed in the error at $n = 90$. Such behaviour is visible in Figure 4b but not at the lower frequency.

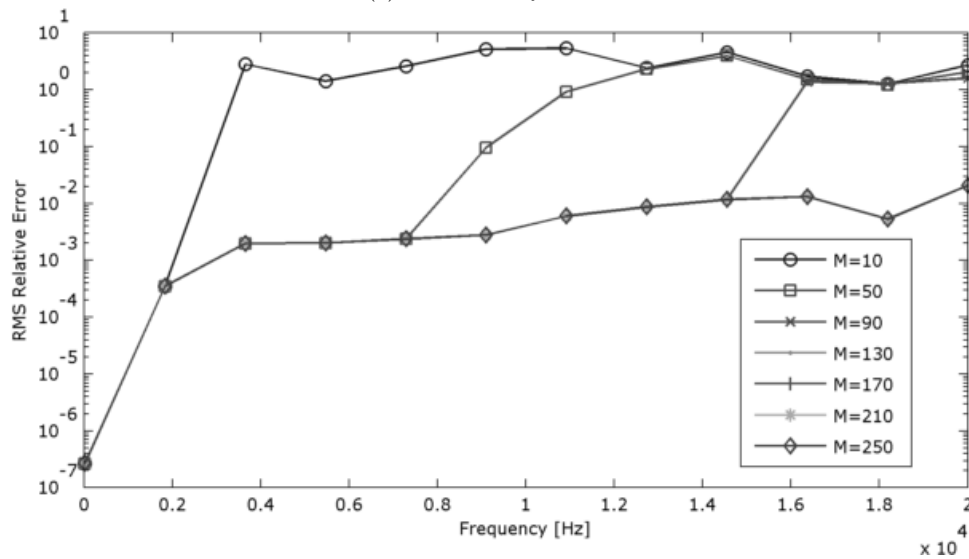
One possible reason for this could be the known phenomenon that the inclusion of an increased number of evanescent modes in the solution forces systems to be near-singular [12]. Such behaviour would easily be amplified through matrix inversion as part of the solution of the linear system. As can be seen from Figure 4b, these error ‘spikes’ may be easily avoided by selecting either a higher (or lower) value for M .

6.1.4 Execution Time

Figure 5 indicates the variation in execution time with mesh density for the highest and lowest frequencies tested. The execution time on MATLAB R2013a decreases with frequency due to the multi-threading of Bessel function evaluation for large arguments. There is negligible variation in the execution time over the range of values of M selected. the value of M has little effect on the execution time. We can assert that this is only true for relatively small values of M (suitable for our application). For larger values, it was found that the extra time needed to compute the DtN boundary condition influences execution time at least as much as the mesh density. The reduction in



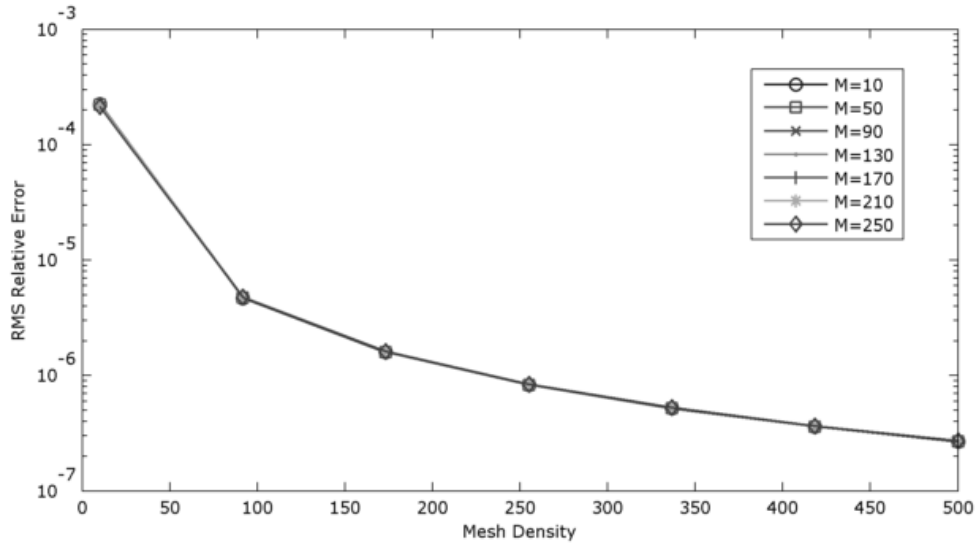
(a) Mesh Density $n = 10$



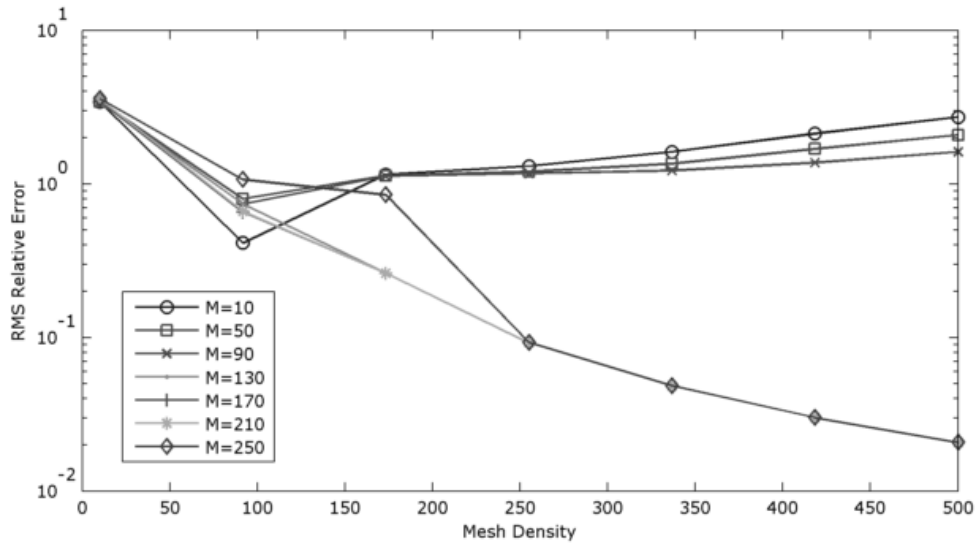
(b) Mesh Density $n = 500$

Figure 3 – Variation in RMS relative error with frequency f and terms in the DtN boundary expansion M for selected mesh densities n .

execution time with frequency is also observable. The rapid increase in execution time with mesh density means that between the last two mesh densities considered, execution time increases by half as much again for a gain in accuracy of just 0.5% at the highest frequency. At the lower frequencies the increase in accuracy is much less as the solution has almost converged to a relative RMS error of the order $10^{-4}\%$.



(a) Frequency $f = 20$ Hz



(b) Frequency $f = 20$ kHz

Figure 4 – Variation in RMS relative error with mesh density n and terms in the DtN boundary expansion M for selected frequencies f .

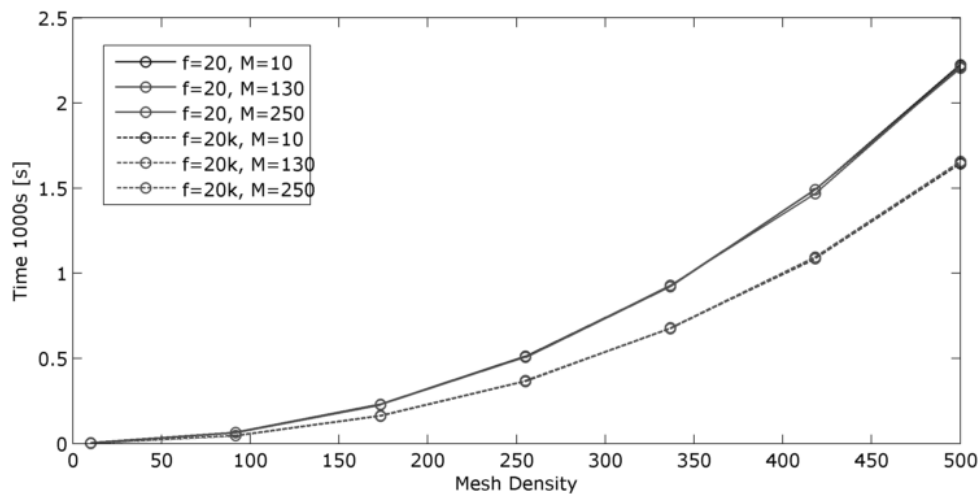


Figure 5 – Variation in execution time with mesh density for $f = 20$ Hz and $f = 20$ kHz for range of M

7. SUMMARY

We have shown that the BEM is a suitable means of accurately computing an acoustic Green's function for a class of 2D geometries. This calculation is accomplished through the solution of the singular form of the governing BVP including the boundary conditions associated with the original problem. Where artificial (transparent or non-reflecting) boundary conditions are required to close the originally semi-infinite domain, we have circumvented the potential under-determination of the system of boundary equations by utilising a Dirichlet-to-Neumann operator to provide the necessary additional equations. The use of constant elements for the BEM greatly simplifies the implementation by avoiding the need for additional numerical integration of the DtN expansion. Multi-threading has also been used to increase efficiency at higher frequencies. The validation exercises compare the numerical results with analytical solutions. Excellent agreement is achieved with relative errors of less than 1%. The DtN boundary condition may be easily extended to other geometries by simply changing the form of the series solution used to construct the DtN operator, with the implementation largely unchanged.

ACKNOWLEDGEMENTS

The work was completed as part of the first author's doctorate degree, supervised by the second author and funded by the alumni of the University of Manchester through Your Manchester Fund. This material has subsequently been extended and has been submitted to Applied Mathematical Modelling for consideration.

REFERENCES

1. Gloerfelt X, Bailly C, Juvé D. Direct computation of the noise radiated by a subsonic cavity flow and application of integral methods. *Journal of Sound and Vibration*. 2003;266(1):119–146.
2. Singer BA, Lockard DP, Lilley GM. Hybrid acoustic predictions. *Computers & Mathematics with Applications*. 2003;46(4):647–669.
3. Howe MS. *Theory of Vortex Sound*. Cambridge: Cambridge University Press; 2003.
4. Keller JB, Givoli D. Exact non-reflecting boundary conditions. *Journal of Computational Physics*. 1989;82(1):172–192.
5. Zienkiewicz OC, Kelly DW, Bettess P. The coupling of the finite element method and boundary solution procedures. *International Journal for Numerical Methods in Engineering*. 1977;11(2):355–375.
6. Zaman SI. A Comprehensive Review of Boundary Integral Formulations of Acoustic Scattering Problems. *Science and Technology Special Review*. 2000;p. 281–310.
7. Harari I, Patlashenko I, Givoli D. Dirichlet-to-Neumann Maps for Unbounded Wave Guides. *Journal of Computational Physics*. 1998;143(1):200 – 223.
8. Grote MJ, Keller JB. On Nonreflecting Boundary Conditions. *Journal of Computational Physics*. 1995;122(2):231–243.
9. Grote M, Keller J. Exact Nonreflecting Boundary Conditions for the Time Dependent Wave Equation. *SIAM Journal on Applied Mathematics*. 1995;55(2):280–297.
10. Linton CM. The Green's Function for the Two-Dimensional Helmholtz Equation in Periodic Domains. *Journal of Engineering Mathematics*. 1998;33(4):377–401.
11. Sandberg RD, Jones LE. Direct Numerical Simulations of Airfoil Self-Noise. *ERCOFTAC Bulletin 90, March, Special Issues in Aeroacoustics (Invited)*. 2012;p. 4–9.
12. Duan W. *Acoustic signals for fluid-filled pipeline blockage detection*. The University of Manchester. Manchester; 2010.